COMMUNICATION

Check for updates

Optimisation of oxide-ion conductivity in acceptor-doped $Na_{0.5}Bi_{0.5}TiO_3$ perovskite: approaching the limit?†

F. Yang, [ID] *[a] M. Li, [ID] [b] L. Li, [ID] [a] P. Wu,[a] E. Pradal-Velázque[a] and D. C. Sinclair [ID] *[a]

$Na_{0.5}Bi_{0.5}TiO_3$ (NBT) perovskite is often considered as a potential lead-free piezoelectric material but it can also be an excellent oxide-ion conductor (M. Li *et al.*, *Nature Materials*, 13, 2014, 31–35). Here we report the non-stoichiometry and oxide-ion conductivity of undoped and acceptor-doped NBT. A range of acceptor-type ions with varying doping levels are selected to incorporate into NBT or Bi-deficient NBT (nominal $Na_{0.5}Bi_{0.49}TiO_{2.985}$; $NB_{0.49}T$). Low levels of acceptors (typically < 2 at%) can be doped on both cation sites of NBT by an ionic compensation mechanism to create oxygen vacancies and are therefore effective in enhancing the bulk oxide-ion conductivity to values of ~2 mS cm^{-1} at 400 °C. A maximum enhancement of less than 1 order of magnitude is achieved using either A-site Sr (or Ca) or B-site Mg doping in $NB_{0.49}T$. This conductivity maximum is in good agreement with an oxygen-vacancy diffusivity limit model in a perovskite lattice proposed by R. A. De Souza (*Advanced Functional Materials*, 25, 2015, 6326–6342) and suggests that optimisation of the ionic conductivity in NBT has been achieved. Our findings on NBT illustrate that this approach should be applicable to other acceptor-doped perovskite oxides to determine their electrolyte (oxide-ion) conductivity limit.

Solid oxide fuel cells (SOFCs) are electrochemical devices that offer an efficient source of electrical power *via* oxidation of a fuel source. In attempts to drive down the operating temperatures of SOFCs from 800 to below 600 °C to reduce start-up times and to improve device lifetime there is a need to develop new oxide-ion solid electrolytes with higher conductivity at these lower temperatures. Acceptor-doped perovskites-based materials such as $(La_{1-x}Sr_x)(Ga_{1-y}Mg_y)O_{3-x/2-y/2}$ (LSGM) and more recently $Na_{0.5}Bi_{0.5}Ti_{1-x}Mg_xO_{3-x}$ are two candidate materials that have

aDepartment of Materials Science & Engineering, University of Sheffield, Mappin Street, Sheffield, S1 3JD, UK. E-mail: fan.yang@sheffield.ac.uk; d.c.sinclair@sheffield.ac.uk

bDepartment of Mechanical, Materials and Manufacturing Engineering, University of Nottingham, NG7 2RD, UK

† Electronic supplementary information (ESI) available. See DOI: 10.1039/c7ta07667c

been investigated as electrolytes for Intermediate Temperature SOFCs (IT-SOFCs). De Souza recently reviewed oxygen vacancy diffusion in a wide variety of ABO_3-type perovskites ranging from ferroelectric dielectrics such as $BaTiO_3$ and mixed ionic-electronic conductors such as $(Ba_{0.5}Sr_{0.5})(Co_{0.8}Fe_{0.2})O_{3-\delta}$ to electrolytes such as $(La_{0.9}Sr_{0.1})(Ga_{0.8}Mg_{0.2})O_{2.85}$. He reported a surprising result that regardless of the level of oxygen vacancies in these materials, the oxygen vacancy diffusivity is very similar and considered the possibility of a fundamental limit to oxygen-vacancy diffusivity in the ABO_3 perovskite lattice. Although unable to conclude a definitive answer to this question, De Souza estimated a plausible limit and reasoned that if the activation entropy of vacancy migration was not higher than $-k_B$ (where k_B is the Boltzmann constant and for a Debye frequency of 10^{13} Hz) then we may be close to the physical limit for the oxygen diffusion coefficient in acceptor-doped cubic perovskites. Here we have attempted to optimise the oxide-ion conductivity in the recently reported $Na_{0.5}Bi_{0.5}TiO_3$ (NBT) oxide-ion conductors by acceptor doping and found that the highest bulk conductivity obtained is consistent with the value calculated from this upper limit, therefore suggesting optimisation of oxide-ion conductivity in this lattice may have been achieved. This approach may be beneficial in trying to establish the optimisation of electrolyte conductivity in a variety of acceptor-doped perovskites and therefore help in the design and development of oxide-ion conductors based on this important class of solids for applications in electrochemical devices such as IT-SOFCs.

The ferroelectric perovskite sodium bismuth titanate, NBT has long been considered as one of the more favoured lead-free piezoelectric materials to replace lead zirconate titanate (PZT).[1–3] It is also a recently discovered oxide-ion conductor with the bulk conductivity (σ_b) of undoped nominally stoichiometric NBT approaching 1.0×10^{-3} S cm^{-1} at 600 °C, which is more than three orders of magnitude higher than that of undoped $LaGaO_3$ at the same temperature.[4–6] It is therefore a promising material to achieve higher oxide-ion conductivity and to develop a family of oxide-ion conductors based on NBT.

The level of non-stoichiometry that can give rise to the high oxide-ion conductivity is low and the defect chemistry and conduction mechanism(s) remain a challenging topic, especially given the complex polymorphism that exists in NBT. The oxide-ion conductivity in nominally stoichiometric NBT, *i.e.* $Na_{0.5}Bi_{0.5}TiO_3$, is attributed to oxygen vacancies generated by low levels of Bi_2O_3 loss during ceramic processing according to

$$2Bi_{Bi}^{\times} + 3O_O^{\times} \xrightarrow{-Bi_2O_3} 2V_{Bi}''' + 3V_O^{\cdot\cdot}, \tag{1}$$
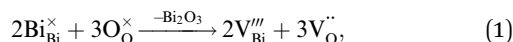
as well as the high oxygen ion mobility associated with highly polarised Bi^{3+} ions and weak Bi–O bonds.[4,5,7] The predominant oxide-ion conduction (as opposed to sodium ion or electronic conduction) in NBT was confirmed by; (i) electromotive force (EMF) measurements, which showed an oxide-ion transport number $t_{ion} > 0.9$ at 600–700 °C and (ii) ^{18}O Time-of-Flight Secondary Ion Mass Spectroscopy (ToF SIMS) where the conductivity calculated by the Nernst–Einstein equation using the diffusion coefficient (D^*) obtained by ^{18}O tracer diffusion measurements was in agreement with the total conductivity of NBT obtained from impedance spectroscopy.[4]

Our previous research showed that enhancement of σ_b can be achieved by inducing a low level of Bi-deficiency in NBT (*e.g.*, nominal $Na_{0.5}Bi_{0.49}TiO_3$; $NB_{0.49}T$) and/or by altering the Na/Bi nominal ratio in the starting compositions prior to processing. $NB_{0.49}T$ has σ_b of ~half an order of magnitude higher than NBT with $t_{ion} > 0.9$ at 600–700 °C.[4] The enhanced σ_b is due to creation of additional oxygen vacancies, as described by eqn (1). At 500 °C, σ_b of $NB_{0.49}T$ is ~1.1×10^{-3} S cm^{-1}, which is above the minimum conductivity requirement for a 1 μm electrolyte in SOFCs.[8] A small amount of Na, Ti-rich secondary phase can be detected in $NB_{0.49}T$ under SEM.[4,9] Further Bi-deficiency (*i.e.* nominal $Na_{0.5}Bi_{0.48}TiO_3$; $NB_{0.48}T$) yields slightly higher σ_b but with a greater proportion of secondary phases. Instead of further increasing the Bi-deficiency level from $NB_{0.49}T$ to $NB_{0.48}T$ with the introduction of significant secondary phases, alternative approaches are required to enhance the oxide-ion conductivity of NBT. It should be stressed the level of A-site non-stoichiometry in undoped NBT is low and under our conditions of ceramic processing undoped compositions with Na/Bi starting ratios ≥ 1 are required to obtain high levels of oxide-ion conductivity.
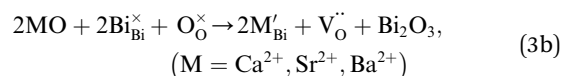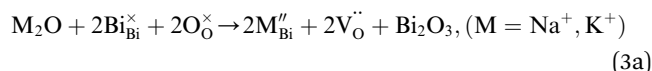
Acceptor doping is a commonly employed strategy to enhance ionic conductivity in fluorite-type (*i.e.*, Y-doped ZrO_2 and Gd-doped CeO_2) and perovskite-type (*i.e.*, Sr, Mg-co-doped $LaGaO_3$) oxide-ion conductors by creating oxygen vacancies. However, the influence of acceptor-doping on the electrical properties in many perovskite titanates, *e.g.*, $BaTiO_3$ (BT) and $SrTiO_3$ (ST) is often more complex with either n-type, p-type or oxide-ion conductivity being dominant depending on a combination of the oxygen-partial-pressure, annealing temperature and cooling rate conditions employed.[10–12] Furnace cooled, acceptor-doped BT and ST ceramics processed in air usually exhibit p-type hole conduction (h$^{\cdot}$) based on the uptake of oxygen (on cooling) as given by the following mechanism
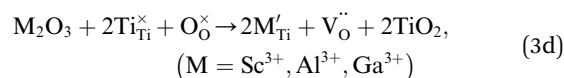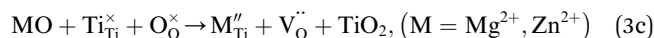
$$V_O^{\cdot\cdot} + \frac{1}{2}O_2 \rightarrow O_O^{\times} + 2h^{\cdot}. \tag{2}$$
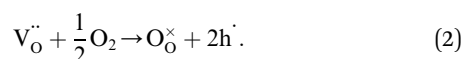
Here we report the oxide-ion conductivity of acceptor-doped NBT and $NB_{0.49}T$ based on various acceptor-type ions (with varying doping levels), *i.e.*, Na$^+$, K$^+$, Ca^{2+}, Sr^{2+}, Ba^{2+} (to replace Bi^{3+} on A-site) and Mg^{2+}, Zn^{2+}, Sc^{3+}, Al^{3+} and Ga^{3+} (to replace Ti^{4+} on B-site). Transition metal ions such as Fe^{3+}, Co^{3+} and Ni^{2+} may introduce electronic conduction into NBT and are therefore not included in this study. Possible compensation mechanisms and the effect of acceptor-doping on the electrical conductivity of NBT are discussed. The results are consistent with the De Souza suggestion that we may be approaching a physical limit of oxygen-diffusion (at least for these acceptor-doped NBT-based perovskites) and the σ_b values reported herein represent close to optimised levels.

NBT has an ABO$_3$ perovskite structure where the A-site is shared by randomly distributed Na$^+$ and Bi^{3+} ions and the B-site is occupied by Ti^{4+} ions. Depending on the ionic size, acceptor-type dopants can be doped either on the A-site to replace Bi^{3+} (larger dopant ions) or on the B-site to replace Ti^{4+} (smaller dopant ions). In each case, doping may occur by either an ionic or electronic compensation mechanism. In the case of the former, acceptor doping would create oxygen vacancies. A summary of the defect reactions investigated for a range of A- and B-site acceptor dopants in this study (given in brackets) are described by the following Kroger–Vink equations:

A-site:

$$M_2O + 2Bi_{Bi}^{\times} + 2O_O^{\times} \rightarrow 2M_{Bi}'' + 2V_O^{\cdot\cdot} + Bi_2O_3, (M = Na^+, K^+) \tag{3a}$$

$$2MO + 2Bi_{Bi}^{\times} + O_O^{\times} \rightarrow 2M_{Bi}' + V_O^{\cdot\cdot} + Bi_2O_3, \\ (M = Ca^{2+}, Sr^{2+}, Ba^{2+}) \tag{3b}$$

B-site:

$$MO + Ti_{Ti}^{\times} + O_O^{\times} \rightarrow M_{Ti}'' + V_O^{\cdot\cdot} + TiO_2, (M = Mg^{2+}, Zn^{2+}) \tag{3c}$$

$$M_2O_3 + 2Ti_{Ti}^{\times} + O_O^{\times} \rightarrow 2M_{Ti}' + V_O^{\cdot\cdot} + 2TiO_2, \\ (M = Sc^{3+}, Al^{3+}, Ga^{3+}) \tag{3d}$$

Although electronic doping may occur due to eqn (2) as observed for many other titanate-based perovskites, impedance spectroscopy and EMF measurements on Sr-doped and Mg-doped $NB_{0.49}T$ in various atmospheres have shown an enhanced pO$_2$-independent σ_b and a higher t_{ion} compared to $NB_{0.49}T$ (Table S1†). These electrical properties prove that acceptor-doping of $NB_{0.49}T$ on both sites is predominantly by an ionic compensation mechanism to create oxygen vacancies (eqn (3)). Acceptor-doping is therefore effective to enhance oxide-ion conduction of $NB_{0.49}T$ without introducing any significant electronic contribution.

Based on the above understanding, various acceptor-type dopants have been selected to dope NBT and $NB_{0.49}T$ in an attempt to optimise the oxide-ion conductivity in this perovskite. Among all the dopants and doping levels investigated in this work, 2% Sr doping on the A-site (nominal $Na_{0.5}Bi_{0.47}Sr_{0.02}TiO_{2.975}$) and 1% Mg doping on the B-site ($Na_{0.5}Bi_{0.49}Ti_{0.99}Mg_{0.01}O_{2.975}$) show

This journal is © The Royal Society of Chemistry 2017

J. Mater. Chem. A, 2017, **5**, 21658–21662 | **21659**

a maximum enhancement of σ_b less than 1 order of magnitude compared to $NB_{0.49}T$, Fig. 1. General features are that higher σ_b is obtained for equivalent doping of $NB_{0.49}T$ (Bi-deficient) compared to NBT (stoichiometric) compositions and that A-site doping can promote higher levels of σ_b compared to B-site doping. Bulk conductivity, σ_b, of $NB_{0.49}T$ with other dopants are all within the shaded region of Fig. 1. Values of σ_b at selected temperatures and activation energies of each composition are listed in Table S2.†

There are several reasons for the limited enhancement of σ_b by acceptor doping. First, the solid solution limit of these dopants in $NB_{0.49}T$ is very low (typically < 2 at%). For example, $Na_2Ti_6O_{13}$ and $MgTiO_3$ secondary phases were detected by SEM for 2% Sr-doped $NB_{0.49}T$ and 2% Mg-doped $NB_{0.49}T$, respectively (Fig. S1†). Second, although acceptor doping increases the oxygen vacancy concentration, it decreases the mobility of charge carriers by increasing the oxygen migration barriers. First-principle calculations have shown that B-site doping, such as Mg^{2+} for Ti^{4+}, significantly increases the oxygen migration barriers by binding with oxygen vacancies.[16] For A-site doping, such as Sr^{2+} for Bi^{3+}, the mobility of oxygen ions is restricted by the lower polarisability and higher bonding strength with oxygen of Sr^{2+} as compared to Bi^{3+}.[9] Third, using the oxygen-vacancy diffusivity limit in a cubic ABO_3 perovskite lattice proposed by R. A. De Souza,[11] an upper limit for σ_b of NBT with oxygen deficiency of 0.025, calculated from Nernst–Einstein equation, is predicted, as shown by the dash line in Fig. 1. At >300 °C, the highest σ_b obtained by A-site Sr-doping and B-site Mg-doping is very close to the upper limit. As a consequence of the reasons given above, it is questionable that further enhancement of σ_b can be achieved by increasing the doping level, either on the A-site or the B-site, as shown in Fig. 2.
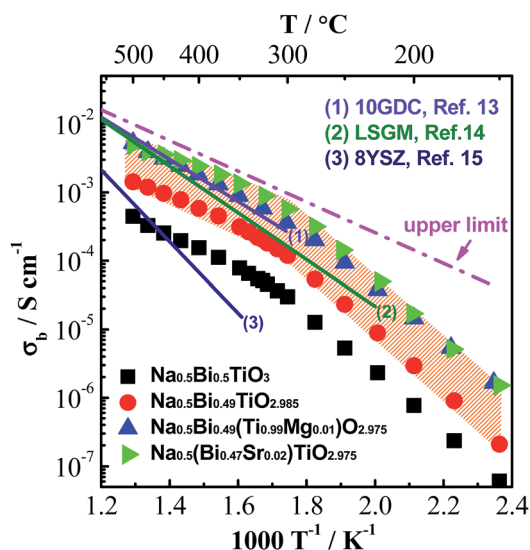

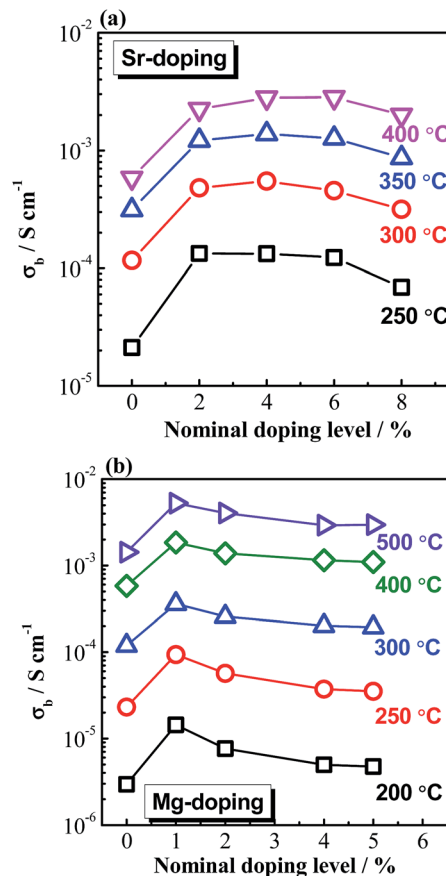
Fig. 2 Bulk conductivity, σ_b, *versus* nominal doping level at selected temperatures: (a) A-site Sr-doped $NB_{0.49}T$, nominal composition $Na_{0.5}Bi_{0.49-x}Sr_xTiO_{2.985-0.5x}$ (x = 0, 0.02, 0.04, 0.06, 0.08) and (b) B-site Mg-doped $NB_{0.49}T$, nominal composition $Na_{0.5}Bi_{0.49}Ti_{1-x}Mg_x$-$O_{2.985-x}$ (x = 0, 0.01, 0.02, 0.04, 0.05).

It is worth mentioning that the $\log_{10} \sigma_b - 1/T$ relationship of undoped and acceptor-doped $NB_{0.49}T$ shows a change in activation energy, E_a from ~0.4 eV above 300 °C to ~0.9 eV below 300 °C (Fig. 1 and Table S2†). The reason(s) for a change of E_a around this temperature has not been fully established but the possibility of a change in charge carrier from oxygen ions to electrons, holes or protons has been excluded. First, impedance spectroscopy measurements in flowing N_2, air and O_2 show a pO_2-independent bulk response, indicating the absence of any significant electronic conduction (Fig. S2†). Second, impedance measurements performed in wet and dry atmospheres, as well as on heating and cooling, show there is no change to σ_b, indicating there is no significant level of protonic conduction (Fig. S3†). Sodium ions are not likely to be charge carriers as there is no open framework (as in NASICON[17]) or Na-layers (as in P2-type Na_xCoO_2 (ref. 18)) in the NBT structure to provide pathways for Na^+. Therefore, it is reasonable to propose the electrical conduction is still dominated by oxygen ions at temperatures below 300 °C. A plausible explanation for the change of E_a is the coexistence of rhombohedral (R) and tetragonal (T) phases in the temperature range from 250 to 400 °C, which was revealed by variable temperature neutron

Fig. 1 An Arrhenius plot of bulk conductivity, σ_b, for undoped and acceptor-doped NBT ceramics. The dash-dot line represents the upper limit of σ_b based on the oxygen-vacancy diffusion coefficient predicted in ref. 11, see text. σ_b for some of the best-known oxide-ion conductors are plotted for comparison: (1) $Ce_{0.9}Gd_{0.1}O_{1.95}$, 10GDC;[13] (2) $La_{0.9}Sr_{0.1}Ga_{0.9}Mg_{0.1}O_{2.9}$, LSGM;[14] (3) $Zr_{0.852}Y_{0.148}O_{1.926}$, 8YSZ.[15] σ_b for $NB_{0.49}T$ with other dopants studied in this work lie within the shaded area.

21660 | *J. Mater. Chem. A*, 2017, **5**, 21658–21662

This journal is © The Royal Society of Chemistry 2017

diffraction studies (Fig. S4†). An estimation of σ_b from the Maxwell model for a two-phase composite showed good agreement with the experimental data of σ_b, suggesting coexistence of R and T phases may be a plausible explanation for the change in E_a at ~300 °C.[19] Other possible reasons for the change of E_a are dissociation of defect clusters and/or changing of conduction paths as recently proposed by Meyer and Albe.[20]

Nevertheless, acceptor-doped $NB_{0.49}T$ still shows attractive bulk conductivity. At 500 °C, σ_b of 2% Sr-doped or 1% Mg-doped $NB_{0.49}T$ is ~5.0 × 10⁻³ S cm⁻¹, which is comparable to LSMG and GDC. Comparing with the two best known δ-Bi_2O_3 oxide-ion conductors, $(BiO_{1.5})_{0.8}(ErO_{1.5})_{0.2}$, 20ESB and $(BiO_{1.5})_{0.88}(DyO_{1.5})_{0.08}(WO_3)_{0.04}$, 8D4WSB, although σ_b of doped $NB_{0.49}T$ is initially lower than 20ESB and 8D4WSB, it shows no appreciable degradation with time contrary to the rapid conductivity degradation of 20ESB and 8D4WSB.[19] After 50 hours, σ_b of Sr-doped $NB_{0.49}T$ is 3 times higher than that of 20ESB and 8D4WSB (Table S3†).

As σ_b appears to be approaching an upper limit, further improvement of electrical conductivity of doped NBT ceramics should be focused on the contributions from grain boundaries (GB's). A typical Z^* plot for conducting NBT is shown in Fig. 3a and displays three (or more, depending on temperature and frequency range) arcs, from left to right (high frequency to low frequency), corresponding to the responses from the bulk, GB and electrodes, respectively. The GB's have a significant contribution to (and sometimes dominate) the overall ceramic membrane resistance. Using an equivalent circuit of three resistor-constant phase elements (R-CPE) connected in series to fit the impedance data, resistance and capacitance of the GB's can be obtained. Assuming the permittivity of the GB's is approximately the same as that of the bulk,[21] a specific GB conductivity (σ_{GB}) can be calculated according to[22]

$$\sigma_{GB} = \frac{1}{R_{GB}} \frac{C_b}{C_{GB}} \frac{t}{A}, \qquad (4)$$

where t and A are the thickness and surface area of the ceramic, respectively and R_{GB}, C_{GB} and C_b are the grain boundary resistance, gain boundary capacitance and bulk capacitance, respectively. As shown in Fig. 3b, σ_{GB} is ~2–3 orders of magnitude lower than σ_b. Ionically blocking GB's in zirconia and ceria-based oxide-ion conductors have been studied for many years and are attributed mainly to impurity segregation at the GB's and/or space charge effects.[21] A consequence of the resistive GB's is that the total conductivity, σ_{tot}, is usually lower than σ_b. An investigation into the GB conductivity and its conduction mechanism(s) is in progress with the aim of minimising the GB contribution to the total conductivity of NBT-based ceramics.

The total conductivity of 2% Sr-doped $NB_{0.49}T$ is higher than 1.0 × 10⁻³ S cm⁻¹ at temperatures > 450 °C, as shown in Fig. 3b. Our previous studies have shown that Sr-doped $NB_{0.49}T$ can withstand 5% H_2/95% N_2 at 550 °C without decomposition.[8,18] Similar behaviour has been observed in Ca-doped $NB_{0.49}T$ (not shown). Mg-doped NBT showed even better stability in reducing atmospheres. Impedance measurements showed no change in the bulk response at 600 °C in 5% H_2/95% N_2 for 45 h with 1%
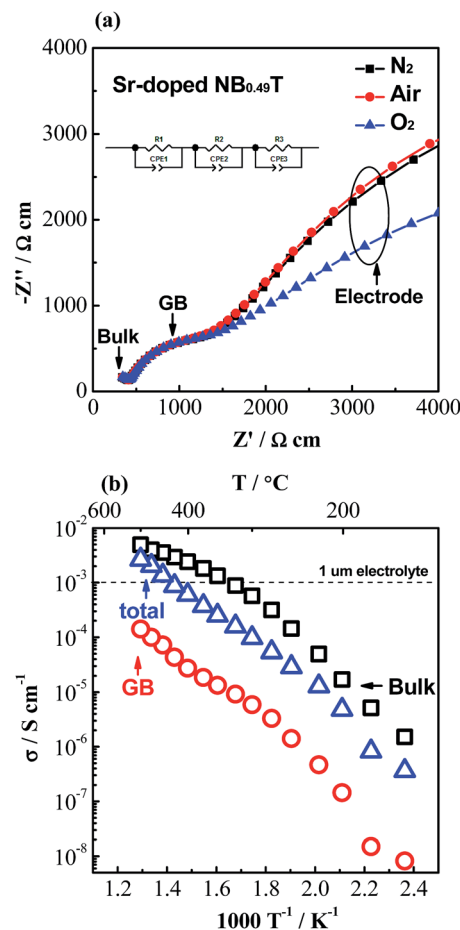

Fig. 3 (a) Complex impedance, Z^*, plots for 2% Sr-doped $NB_{0.49}T$ with Pt electrodes under different atmospheres at 400 °C; the inset figure is the equivalent circuit used to fit the impedance data. (b) Arrhenius plots for σ_b, σ_{GB} and σ_{tot} for 2% Sr-doped $NB_{0.49}T$. The horizontal dash line indicates the minimum conductivity requirement for a 1 μm electrolyte for SOFCs.[8]

Mg-doped NBT in contrast to a significant reduction of the bulk response for undoped NBT under the same conditions.[4] These doped NBT materials are therefore very promising to be used as an electrolyte in SOFCs working in the temperature range of 450–550 °C.

In conclusion, low levels of acceptor-type dopants either on the A-site to replace Bi^{3+} or on the B-site to replace Ti^{4+} can be used to create additional oxygen vacancies and therefore enhance the ionic conductivity of NBT (or $NB_{0.49}T$). Among all the doping elements investigated in this work, Sr- or Ca-doping on A-site and Mg-doping on B-site are the most effective dopants to enhance σ_b; however, it does appear to be reaching a limit consistent with that proposed by De Souza. These acceptor-doped $NB_{0.49}T$ show excellent ionic conductivity with extremely low levels of degradation and reasonable stability in reducing atmosphere. They also have an advantage over δ-Bi_2O_3 oxide-ion conductors as being more sustainable (rare-earth free) materials with lower Bi-contents. Further work will be focused on understanding the grain boundary conductivity and conduction mechanism to minimise their contribution to the

This journal is © The Royal Society of Chemistry 2017

J. Mater. Chem. A, 2017, **5**, 21658–21662 | **21661**

total conductivity of NBT-based oxide-ion conducting ceramics. The significance of this work is not only understanding the defect chemistry by acceptor doping of NBT and optimising its oxide-ion conductivity, but also trying to establish the upper limit of electrolyte conductivity in a variety of acceptor-doped perovskites from the oxygen vacancy diffusivity limit, which is determined mainly by the structural parameters of the host. The upper limit of conductivity is the highest value that can be achieved by acceptor doping, which can give a guideline whether optimisation of conductivity is achieved and will therefore help in the design and development of oxide ion conductors.

Conflicts of interest

There are no conflicts to declare.

Acknowledgements

References

1 E. Aksel and J. L. Jones, *Sensors*, 2010, **10**, 1935.
2 D. Damjanovic, N. Klein, J. Lin and V. Porokhonskky, *Funct. Mater. Lett.*, 2010, **3**, 5.
3 K. Reichmann, A. Feteira and M. Li, *Materials*, 2015, **8**, 8467.
4 M. Li, M. J. Pietrowski, R. A. De Souza, H. Zhang, I. M. Reaney, S. N. Cook, J. A. Kilner and D. C. Sinclair, *Nat. Mater.*, 2014, **13**, 31.
5 M. Li, H. Zhang, S. N. Cook, L. Li, J. A. Kilner, I. M. Reaney and D. C. Sinclair, *Chem. Mater.*, 2015, **27**, 629.
6 T. Ishihara, H. Matsuda, M. A. bin Bustam and Y. Takita, *Solid State Ionics*, 1996, **86–88**, 197.
7 D. Schütz, M. Deluca, W. Krauss, A. Feteira, T. Jackson and K. Reichmann, *Adv. Funct. Mater.*, 2010, **22**, 2285.
8 Z. Gao, L. V. Moqni, E. C. Miller, J. G. Railsback and S. A. Barnett, *Energy Environ. Sci.*, 2016, **9**, 1602.
9 F. Yang, P. Wu and D. C. Sinclair, *Solid State Ionics*, 2017, **299**, 38.
10 S. Li, J. Morasch, A. Klein, C. Chirila, L. Pintilie, L. Jia, K. Ellmer, M. Naderer, K. Reichmann, M. Gröting and K. Albe, *Phys. Rev. B: Condens. Matter Mater. Phys.*, 2013, **88**, 045428.
11 R. A. De Souza, *Adv. Funct. Mater.*, 2015, **25**, 6326.
12 D. M. Symth, *J. Electroceram.*, 2003, **11**, 89.
13 T. Zhang, P. Hing, H. Huang and J. A. Kilner, *Solid State Ionics*, 2002, **148**, 567.
14 C. Haavik, E. M. Ottesen, K. Nomura, J. A. Kilner and T. Norby, *Solid State Ionics*, 2004, **174**, 233.
15 Y. Arachi, H. Sakai, O. Yamamoto, Y. Takeda and N. Imanishai, *Solid State Ionics*, 1999, **121**, 133.
16 X. He and Y. Mo, *Phys. Chem. Chem. Phys.*, 2015, **17**, 18035.
17 N. Anantharamulu, K. Koteswara Rao, G. Rambabu, B. Vijaya Kumar, V. Radha and M. Vithal, *J. Mater. Sci.*, 2011, **46**, 2821.
18 R. Berthelot, D. Carlier and C. Delmas, *Nat. Mater.*, 2011, **10**, 74.
19 F. Yang, H. Zhang, L. Li, I. M. Reaney and D. C. Sinclair, *Chem. Mater.*, 2016, **28**, 5269.
20 K.-C. Meyer and K. Albe, *J. Mater. Chem. A*, 2017, **5**, 4368.
21 X. Guo and J. Maier, *J. Electrochem. Soc.*, 2011, **148**, 121.
22 X. Guo and R. Waser, *Prog. Mater. Sci.*, 2006, **51**, 151.

21662 | *J. Mater. Chem. A*, 2017, **5**, 21658–21662

This journal is © The Royal Society of Chemistry 2017